Anomalous diffusion, structural relaxation and shear thinning in glassy hard sphere fluids

2008 J. Phys.: Condens. Matter 20 244129

(http://iopscience.iop.org/0953-8984/20/24/244129)

IOP PUBLISHING JOURNAL OF PHYSICS: CONDENSED MATTER

J. Phys.: Condens. Matter **20** (2008) 244129 (9pp) doi:10.1088/0953-8984/20/24/244129

Anomalous diffusion, structural relaxation and shear thinning in glassy hard sphere fluids

Erica J Saltzman[1], **Galina Yatsenko and Kenneth S Schweizer**[2]

Department of Materials Science, University of Illinois, 1304 West Green Street, Urbana, IL 61801, USA

E-mail: kschweiz@uiuc.edu

Received 26 September 2007, in final form 30 October 2007
Published 29 May 2008
Online at stacks.iop.org/JPhysCM/20/244129

Abstract

The stochastic nonlinear Langevin equation theory of the single-particle dynamics of glassy hard sphere fluids and suspensions has been applied to address several issues raised by recent experimental and simulation studies. The theoretically predicted degree of non-Fickian behaviour at intermediate times, and the slow structural relaxation component of the small wavevector incoherent dynamic structure factor, are compared quantitatively with recent measurements and reveal good agreement. A roughly power law growth, with a common exponent, of the classic and alternative non-Gaussian parameter amplitudes with mean alpha relaxation time is predicted, and qualitative similarities with a multi-point susceptibility that quantifies dynamic heterogeneity effects are noted. The nonlinear rheology version of the theory has been quantitatively applied to explain recent measurements of shear-induced acceleration of the single-particle relaxation time on the local cage scale. The resulting no adjustable parameter calculations are in remarkable agreement with the experimental observations for the absolute magnitude, volume fraction dependence and fractional power law scaling aspects of the shear thinning phenomenon.

(Some figures in this article are in colour only in the electronic version)

1. Introduction

The glassy dynamics of colloidal suspensions and dense fluids composed of hard spheres is an intensely studied problem. Ideal mode-coupling theory (MCT) is a microscopic, force-based description that has made novel predictions based on a literal arrest or 'ideal glass transition' singularity arising from many particle caging [1, 2]. By adjusting the location of the nonergodicity transition good agreement with experiments and simulations for many 'average' properties of hard sphere fluids has been documented [1–3]. However, MCT fails to describe the multiple fluctuation or non-Gaussian aspects corresponding to observables that are either exactly zero if the dynamics is a Gaussian process or exhibit *qualitative* deviations from Gaussian behaviour [4]. The reason is ideal MCT does not address activated transport over barriers, which is probably a dominant factor for dynamically intermittent and heterogeneous processes. Computer simulations based on a variety of dynamical laws all find activated hopping is important even *below* (above) the *empirically* deduced MCT critical volume fraction (temperature) [5–15]. As has been recently critically summarized [4], simulations and confocal microscopy experiments have established that large non-Gaussian dynamical effects occur in the putative glassy precursor regime of hard-sphere-like systems.

Our goal has been to build on MCT to address barriers, activated hopping and strongly non-Gaussian processes. A microscopic and predictive theory for *single-particle* glassy dynamics of hard sphere fluids and suspensions based on a stochastic nonlinear Langevin equation (NLE) and with no singularities below random close packing (RCP) has been proposed by two of us [16]. The volume fraction dependence of the *mean* relaxation time, viscosity and self-diffusion have

[1] Present address: Department of Polymer Science, University of Massachusetts, Amherst, MA 01003, USA.

[2] Author to whom any correspondence should be addressed.

been quasi-analytically computed and are in good agreement with suspension experiments [16, 17]. The quasi-analytic version of the theory has also been successfully generalized to treat the nonlinear rheological response of glassy hard sphere fluids [18, 19].

Non-Gaussian fluctuation effects have been recently studied [4, 20, 21] for the quiescent fluid based on a Brownian trajectory solution of our theory. A host of interrelated and strong non-MCT fluctuation effects, of a purely dynamical origin, are predicted due to the intermittent nature of particle trajectories and the attendant *broad distribution* of relaxation times. Relevant highlights include the following [20–22]. (i) Strong decoupling for volume fractions $\phi > 0.5$ of the self-diffusion constant, D, and single-particle alpha relaxation time, $\tau^* = \tau(q^*)$, as defined from the incoherent dynamic structure factor, $F_s(q,t)$, at the wavevector corresponding to the peak of the static structure factor $S(q)$. (ii) A spatial scale dependence of the decoupling of diffusion and relaxation characterized by a Fickian crossover length scale ξ_D that increases linearly with volume fraction and is related to the decoupling factor as $\xi_D \propto \sqrt{D\tau^*}$. (iii) Dynamic scaling is predicted for all volume fractions and wavevectors ($q\sigma \sim 2.6$–13) studied in the sense that the quantity $X(q) \equiv \tau(q)D/(\tau(q)D)_0$ (where $(\tau(q)D)_0$ is the normal fluid value) collapses as $X \simeq 1 + c(q\xi_D)^\nu$, where c is a constant and $\nu \simeq 1.7 \pm 0.2$, in agreement with simulation [23]. (iv) The amplitudes of two distinct non-Gaussian parameters that quantify heterogeneous dynamics on the late β and final α timescales, respectively, grow strongly with volume fraction. (v) As the barrier increases the real space particle displacement distribution function broadens from Gaussian in the normal fluid regime to an increasingly bimodal form at intermediate times and high volume fractions.

The above and other predictions compare favourably with experiments and simulations. Hence, we have argued that the rich single-particle mean and fluctuation dynamics of simple fluids in the glassy precursor regime can both be understood from the elementary process of cage escape and activated hopping on the particle length scale [4, 20–22]. In the present article we extend our theory for both quiescent and sheared hard sphere fluids to address three areas of recent experimental measurement: (1) Additional analysis of anomalous diffusion and non-Gaussian effects. (2) Quantification of the structural relaxation component of the decay of the incoherent dynamic structure factor motivated by dynamic light scattering measurements [24, 25]. Computational results for a subset of the eleven volume fractions previously studied are presented for these first two topics. (3) The acceleration of the mean alpha relaxation time at ultrahigh volume fractions under strong shear deformation and quantitative comparison with a very recent experiment [26]. We first briefly review the essential elements of the approach in the linear response regime.

2. Theoretical background

Our theory has been heuristically motivated on physical grounds [16], and derived from time-dependent statistical mechanics [27]. It is built on a locally solid state, or inhomogeneous fluid, picture of slow dynamics. For suspensions, hydrodynamic interactions enter only as they influence the short time/distance dissipative dynamics at the one and two particle level. The interparticle force contribution to the NLE is rendered tractable based on a local equilibrium idea common to dynamic density functional theory approaches [28]. This allows the instantaneous intermolecular forces to be renormalized in an effective potential manner via $S(q)$. Temporal deviations from locally stable initial positions are modelled in an Einstein solid spirit [27, 29]. Dynamic closure at the tagged particle level is achieved based on an approximate relation between one and two particle local dynamics. The resultant closed nonlinear stochastic Langevin equation of motion for the instantaneous scalar particle *displacement* from its initial position, $r(t)$, is given in the overdamped limit by [16, 27]

$$\zeta_s \frac{\partial r(t)}{\partial t} = -\frac{\partial F_{\rm eff}[r(t)]}{\partial r(t)} + \delta f(t), \tag{1}$$

where the random force satisfies $\langle \delta f(0)\delta f(t)\rangle = 2k_BT\zeta_s\delta(t)$, and $\zeta_s = k_BT/D_s$ is the short time friction constant. The latter is accurately computed based on independent binary collisions [30] as $\zeta_s = \zeta_0 g(\sigma)$, where for colloids $\zeta_0 = k_BTD_0^{-1}$ is the dilute solution Stokes–Einstein friction constant, σ is the hard sphere diameter, and an essentially exact expression [17] for the contact value of the radial distribution function, $g(\sigma)$, is employed. The effective or nonequilibrium free energy is

$$F_{\rm eff}(r) = -3\ln(r) - \int \frac{{\rm d}\vec{q}}{(2\pi)^3}\rho C^2(q)S(q)[1+S(q)]^{-1} \times \exp\left[-\frac{q^2r^2}{6}(1+S^{-1}(q))\right] \equiv F_{\rm ideal} + F_{\rm excess}, \tag{2}$$

where $C(q) = (1 - S(q))/\rho$ is the Fourier-transformed direct correlation function calculated using Percus–Yevick theory [31] and ρ is the number density. The nonequilibrium free energy is a monotonically decreasing function of particle displacement below $\phi_c = 0.432$. A local minimum in $F_{\rm eff}(r)$ at $r = r_L$ first emerges at $\phi_c = 0.432$ [16] which defines a simplified ('naive' [29]) MCT nonergodicity transition. In the NLE theory this 'ideal glass transition' signals the onset of transient particle localization, emergence of an entropic barrier of height F_B and a crossover to activated dynamics [16]. The barrier is $\sim k_BT$ at $\phi = 0.5$, and grows to $6.7k_BT$ at $\phi = 0.57$. Unless otherwise stated, all timescales are expressed in units of $\tau_0 = \sigma^2/D_0$.

Equations (1) and (2) are based on a solid-state-like picture of a dense fluid and cannot be valid at arbitrarily long times/displacements. A dynamical crossover to an irreversible linear (three-dimensional) Langevin equation description is invoked by modifying equation (1) as [20, 27]:

$$-\frac{\partial F_{\rm eff}}{\partial r(t)} \to -\zeta_{\rm hop}(\phi)\frac{\partial \vec{r}}{\partial t}. \tag{3}$$

A hopping friction constant is introduced to account for the frictional resistance associated with the barrier crossing

event. To quantitatively implement this idea a cage escape displacement or 'reaction point', $r^\dagger$, is introduced that is *a priori* computed based on a physically motivated criterion for when the localizing cage force becomes irrelevant. All sensible formulations of the reaction point idea have been shown to yield very similar results, $r^\dagger/\sigma \simeq 0.5$–$0.6$ [20]. The transition in dynamical description is executed on a single-trajectory basis and assumes that after a reaction event trajectory propagation is described by a *unique ensemble averaged* friction constant, $\zeta_s \to \zeta_s + \zeta_{hop}$ where

$$\frac{1}{\zeta_{hop}} = \frac{1}{N}\sum_{i=1}^{N}\frac{1}{\zeta_{hop,i}}. \tag{4}$$

The trajectory friction constant $\zeta_{hop,i} = 6t_i^\dagger/r^{\dagger 2}$, $t_i^\dagger$ is the time for the ith trajectory to pass the reaction point, and the number of trajectories $N = 40\,000$. A 'hopping diffusion constant' is defined as $D_{hop} = k_B T/\zeta_{hop}$, and the long time diffusion constant is given by $D = k_B T/(\zeta_s + \zeta_{hop})$. The recent computational study [20, 21] has been performed for eleven volume fractions in the interval $0.4 \leqslant \phi \leqslant 0.57$.

3. Anomalous diffusion and non-Gaussian effects

The mean square displacement (MSD), $\langle r^2(t)\rangle$, has been previously studied [20]. The degree of anomalous non-Fickian diffusion in the intermediate time caging regime can be described via the minimum value of the effective exponent $\Delta_{min}(\phi)$ in the apparent power law $\langle r^2(t)\rangle \propto t^\Delta$. Our results are shown in figure 1 and have several notable aspects. (i) The volume fraction dependence of Δ_{min} can be described as piecewise linear. (ii) For $\phi < 0.5$ the barrier is either nonexistent or less than the thermal energy and $\Delta_{min}(\phi)$ weakly decreases with volume fraction. (iii) In the $\phi > 0.5$ activated dynamics regime the effective exponent decreases much more rapidly. If the high volume fraction linear behaviour is empirically extrapolated one finds $\Delta_{min} \to 0$ at $\phi \sim 0.575$. This value agrees well with analyses based on fitting ideal MCT to experimental data by adjusting the location of the ideal glass singularity [3, 24], although the exponent is always nonzero below RCP in our approach. The corresponding dynamic light scattering data [25] for $\Delta_{min}(\phi)$ are also shown in figure 1. The measurements were made using a binary mixture formulation and polydisperse colloids of mean diameter ∼400 nm. The observed effective exponent behaviour is in rather remarkable agreement with the *no* adjustable parameter theoretical results.

The inset of figure 1 shows theoretical results for several characteristic displacements as a function of volume fraction [20, 21]: (a) root MSD corresponding to the minimum non-Fickian exponent, R_m, (b) root MSD at the time when the classic non-Gaussian parameter (NGP) [31], $\alpha_2(t) \equiv (3\langle r^4(t)\rangle/5\langle r^2(t)\rangle^2) - 1$, is a maximum, (c) root MSD at the alpha relaxation time τ^*, and (d) location of the maximum of the peak of the fast subpopulation in the displacement distribution function at the alpha relaxation time [21], $P(r,t) \propto r^3 G_s(r,t)$ where $G_s(r,t)$ is the standard van Hove distribution function. The first two length scales

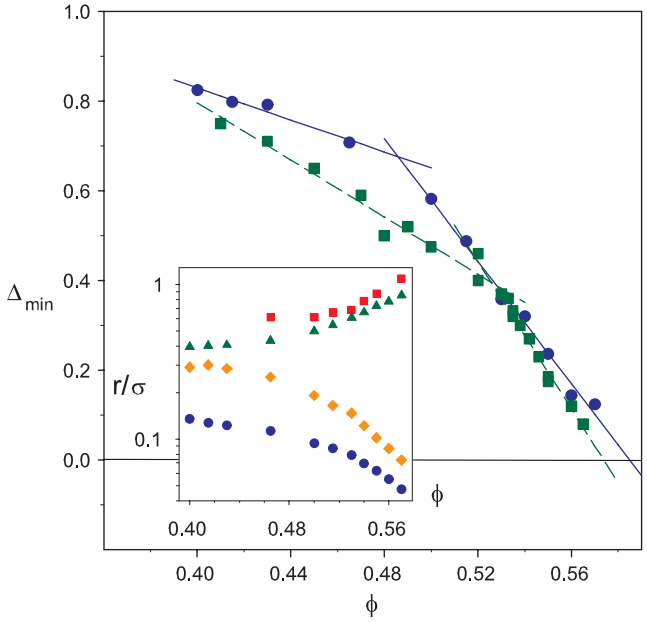

Figure 1. Minimum non-Fickian exponent, Δ_{min}, characterizing the subdiffusive plateau: $\langle r^2\rangle \sim t^{\Delta_{min}}$. The NLE theory results (blue circles) with two linear fits (blue solid lines): $\Delta_{min} \cong -1.8\phi + 1.5$ (low ϕ), $\Delta_{min} \cong -6.8\phi + 4.0$ (high ϕ). Dynamic light scattering results [30] (green squares) with two linear fits (green dashed lines): $\Delta_{min} \cong -3.2\phi + 2.1$ (low ϕ), $\Delta_{min} \cong -8.2\phi + 4.7$ (high ϕ). Inset shows characteristic displacements with respect to volume fraction: root mean square displacement at subdiffusive plateau, R_m (blue circles); root mean square displacement at time of maximum non-Gaussian parameter (orange diamonds); root mean square displacement at alpha relaxation time (green triangles); location of fast peak of displacement distribution at alpha relaxation time (red squares).

are associated with dynamics on the fast beta (transient localized) regime. They decrease with volume fraction, and vary much more rapidly once a significant barrier emerges. The other two lengths quantify displacements on the alpha relaxation timescale and increase with volume fraction. This is the origin of our predicted decoupling of relaxation and diffusion [20, 21], i.e. an increase of $D\tau^*$ with ϕ.

The root mean square displacement corresponding to the subdiffusive plateau, R_m, decreases by a bit more than a factor of two as the volume fraction increases over the wide range of 0.40–0.57 (figure 1 inset). We are aware of two experimental studies of this property for hard sphere colloids. The measurements of van Megen and co-workers [25] find R_m/σ decreases from roughly 0.23 to 0.17 as ϕ increases from 0.50 to 0.56. These values are larger than the theoretical results. The experiments also find R_m tends to saturate at very high volume fractions, in contrast to our calculations. On the other hand, the experiments of Weeks and Weitz [32] find R_m/σ varies from ∼0.16 to 0.046 as ϕ increases from 0.46 to 0.56, in surprisingly good agreement with our calculations. Moreover, the studies of [32] find R_m is a monotonically decreasing function of volume fraction up to, and beyond, $\phi = 0.56$, a trend that differs from the experiments of [25] but which is in agreement with our theoretical predictions.

Two scalar measures of non-Gaussian dynamics on the late beta and alpha relaxation timescales are the classic NGP and

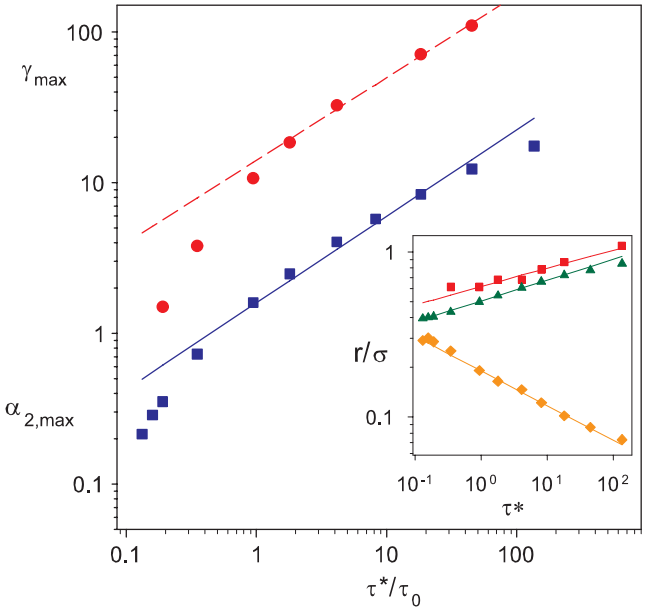

Figure 2. Maximum amplitude of the non-Gaussian parameter $\alpha_{2,\max}$ (blue squares) and alternate non-Gaussian parameter $\gamma_{\max}$ (red circles) as a function of alpha relaxation time with power law fits: $\alpha_{2,\max} \sim (\tau^*)^{0.57}$ (blue solid line); $\gamma_{\max} \sim (\tau^*)^{0.55}$ (red dashed line). Inset shows characteristic displacements as a function of the alpha relaxation time (points) and power law fits $r \sim (\tau^*)^{\gamma}$ (lines): root mean square displacement at the time of maximum NGP (orange diamonds; $\gamma = -0.21$); root mean square displacement at the alpha relaxation time (green triangles; $\gamma = 0.13$); location of fast peak of displacement distribution at alpha relaxation time (red squares; $\gamma = 0.11$).

alternative NGP [33], defined as $\gamma(t) \equiv (\langle 1/3r^2(t)\rangle \langle r^2(t)\rangle) - 1$, respectively. We previously established the magnitude and timescale of the peaks of these different measures of non-Gaussian dynamics as a function of volume fraction [21]. Recently, several simulation studies of four-point dynamical susceptibilities have been performed to characterize the space–time mobility fluctuations. For a binary thermal atomic mixture at intermediate temperatures the amplitude of the four-point susceptibility in the small wavevector limit, $\chi_4(t)$, scales as an apparent power law with the alpha relaxation time, $\chi_{4,\max} \propto (\tau^*)^{0.46}$, a relation reminiscent of dynamic critical phenomena [34]. We are motivated to analyse the dependence of the amplitudes $\alpha_{2,\max}$ and $\gamma_{\max}$ on τ^* by this finding, as well as our previous discovery [21] of a deep connection between the amplitudes of these two non-Gaussian parameters and the similar shapes of the alternate NGP and $\chi_4(t)$. Both the susceptibility [34] and alternate non-Gaussian parameter [21] are asymmetric functions with short time tails and abrupt long time decays, and both peak at roughly the alpha time, which suggests they may reflect similar physics.

Figure 2 presents our results. For small enough τ^* and volume fractions at which the barrier is nonexistent or less than $k_B T$ there is no simple power law dependence. However, as the strongly activated regime is entered both NGP amplitudes follow apparent power laws over roughly 1.5 decades with exponents that are almost the same and slightly larger than 0.5. For the classic NGP there appears to be a bending over to a weaker dependence at the longest relaxation times (highest barriers), a trend also seen in simulations of $\chi_4(t)$ at the lowest accessible temperatures [34]. Of course, our limited range of data precludes definitive statements, but we find the similarities between the NGP parameters' amplitude growth and the behaviour of $\chi_{4,\max}$ to be interesting.

The inset of figure 2 shows three of the characteristic displacements in figure 1 vary with the alpha relaxation time as effective power laws with small apparent exponents. The two growing length scales behave essentially identically to the Fickian crossover length mentioned above which is $\xi_D \propto \sqrt{D\tau^*} \propto (\tau^*)^{0.115}$ in the strongly activated regime [21]. The growth of the MSD at the alpha time as a weak power law of τ^* is also consistent with recent simulations [33, 35]. The behaviour of the displacement at the maximum of the classic NGP is especially striking since power law scaling applies over a three orders of magnitude increase of τ^* that covers the 'normal' fluid regime (where the barrier is zero) and the strongly activated regime. This prediction should be amenable to testing via experiment and computer simulation.

4. Structural relaxation and non-Markovian slow dynamics

Incoherent dynamic structure factor measurements [3] for glassy colloidal suspensions performed at a single wavevector of $q\sigma = 2.6$ have recently been further analysed [25]. A primary goal was to separate the decay of $F_s(q,t)$ into a 'fast' Markovian process and a slower non-Markovian process indicative of structural relaxation. The simplest analysis writes [25]:

$$F_s(q,t) \equiv T(q,t) + N(q,t), \tag{5}$$

where T is the 'thermal mode' given by the Fickian form $T(q,t) = \exp(-q^2 D_s t)$. The short time diffusion constant, D_s, has been experimentally measured [3, 25] and is well described [17, 30] by $D_s = D_0/g(\sigma)$ as employed in our theory. Hence, $N(q,t)$ represents the slow part of the decay associated with the alpha relaxation process. High volume fraction results for $N(q\sigma = 2.6, t)$ are shown in figure 4 of [25] for $\phi = 0.409$, 0.517 and 0.551. Peaks of amplitude ~0.33, 0.8, and 0.95 occur with increasing volume fraction, and the corresponding timescale grows by roughly an order of magnitude.

These experimental results have motivated us to analyse our prior calculations [20, 21] of $F_s(q,t)$ using equation (5). Figure 3 shows $N(q,t)$ at $\phi = 0.55$ for $q = 2.6/\sigma$, q^*, the second peak of the static structure factor q_2, and two wavevectors, q_a and q_b, that are equidistant [20, 21] between q^* and $q = 2.6/\sigma$. Time is nondimensionalized by the Brownian time $\tau_B \equiv \tau_0/24$, as in [25], and the lowest wavevector is the experimental one. The amplitude of $N(q,t)$ for the lowest wavevector is similar to (a bit smaller than) the experimental observations. As wavevector increases the $N(q,t)$ peak shifts to shorter timescales as expected, but the amplitude is nearly constant.

Figure 4(a) presents calculations over a wide range of volume fractions for the relatively low wavevector studied

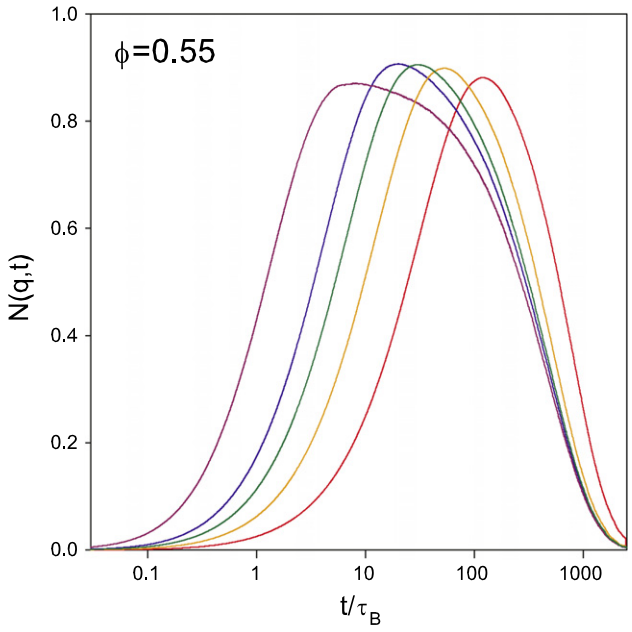

Figure 3. Long time component of the incoherent dynamic structure factor, $N(q, t)$, for $\phi = 0.55$ and wavevectors defined in the text (from right): $q = 2.6/\sigma$, q_a, q_b, q^*, q_2.

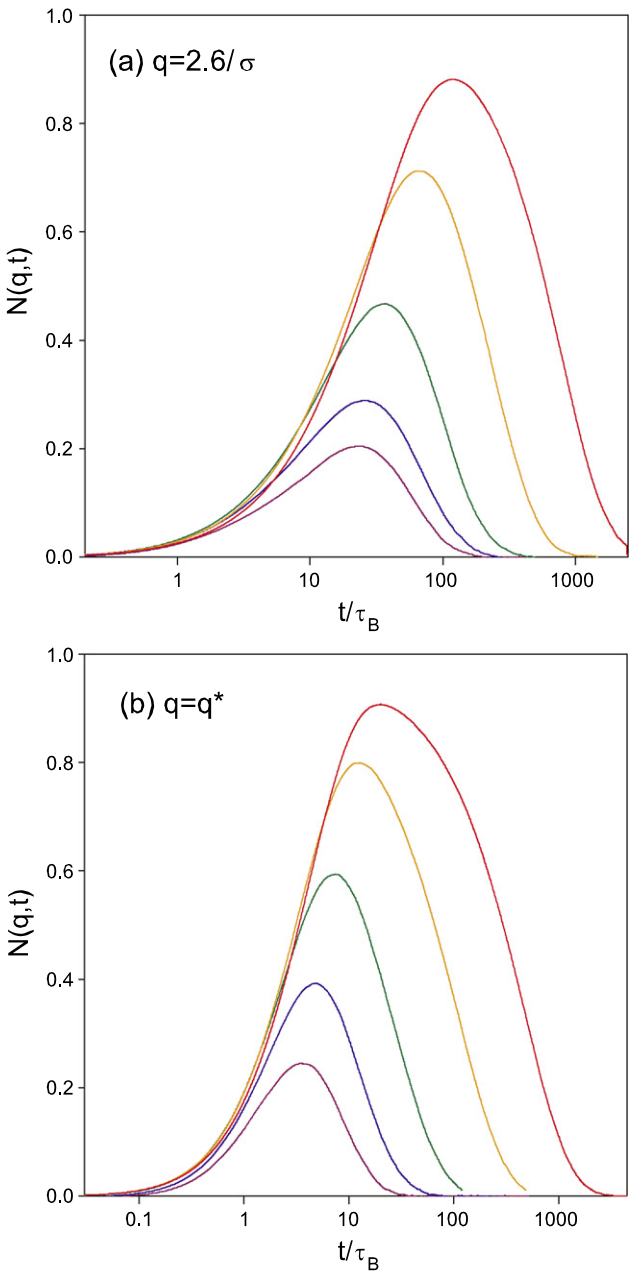

Figure 4. Long time component of the incoherent dynamic structure factor, $N(q, t)$, for (a) $q = 2.6/\sigma$ and (b) $q = q^*$ at (from bottom): $\phi = 0.43, 0.465, 0.5, 0.53, 0.55$.

experimentally [3, 25]. The functions have an amplitude that increases with volume fraction in a manner quite similar to the experimental observations. Figure 4(b) shows the analogous results for the cage scale q^*. The magnitude and volume fraction dependence of the amplitudes, and the shift of the peak time with volume fraction, are all qualitatively the same as in figure 4(a). Of course, the absolute timescales are shorter, and at the highest volume fraction the shape of $N(q^*, t)$ becomes more skewed at long times.

Figure 5 presents various characteristic times, in units of the Brownian time, as a function of volume fraction. The time of the peak of $N(q\sigma = 2.6, t)$ is nearly constant at lower volume fractions and then increases as the dynamics becomes activated. The analogous experimental data are shown as large (indicating the apparent data scatter [25]) circles. Reasonable agreement with theory is found with regards to the absolute magnitude of the timescale and its volume fraction dependence except at the lowest volume fractions where the dynamics in the theory is not activated. In the activated regime the theoretical results are well represented as exponential, varying as $\sim \exp(26.9\phi)$. Curiously, this exponential law, including the numerical factor of $\sim$27, is essentially identical to prior calculations of the glassy shear modulus [36], a property determined by the most localized aspects of the problem. This is another example of connections between dynamical properties on different time and length scales that emerge from the NLE theory [16, 20, 21]. A physical and mathematical understanding of this aspect has been recently developed [37]. Figure 5 also shows that the timescale of the maximum $N(q = q^*, t)$ has the same volume fraction dependence as the timescale of $N(q\sigma = 2.6, t)$, and the peak time of the classic NGP behaves similarly over a restricted range. The timescale of maximum anomalous diffusion is also shown and exhibits a somewhat weaker growth with volume fraction in the activated regime than the other timescales.

Although there are quantitative differences between theory and experiment for $N(q\sigma = 2.6, t)$, overall the level of agreement seems significant especially since there are no adjustable or fitting parameters in the NLE approach. Future experiments would be valuable to test our results for the q-dependence of $N(q, t)$.

5. Shear thinning of the alpha relaxation time

The NLE theory has been generalized to treat the effect of applied stress based on a generalized Eyring-like idea [18].

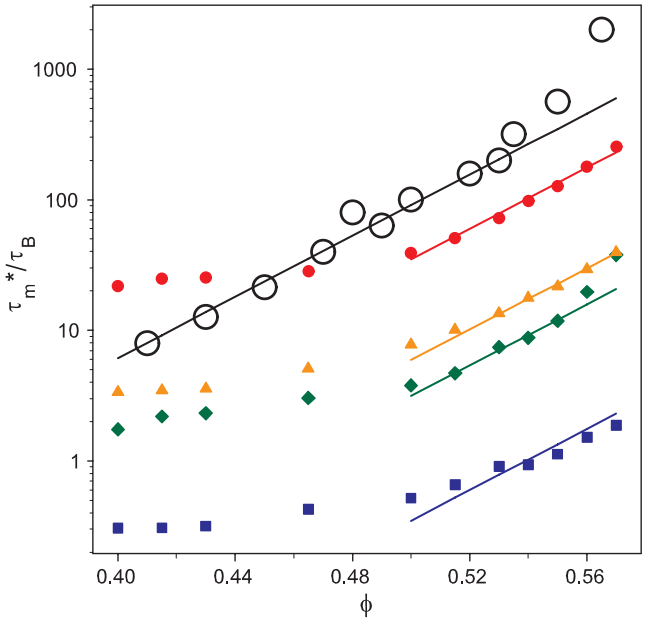

Figure 5. Characteristic timescales in units of the Brownian time. Time of the maximum of $N(q,t)$ for $q = 2.6/\sigma$ (red circles), q^* (orange triangles); analogous dynamic light scattering results [30] for $q = 2.6/\sigma$ (open circles). Time of the maximum non-Gaussian parameter (green diamonds), and maximum non-Fickian behaviour (blue squares). Lines associated with the various points denote an exponential behaviour $\sim \exp(26.9\phi)$.

Specifically, in the presence of a constant stress field, τ, the instantaneous displacement of a particle results in mechanical work which reduces the barrier and accelerates motion. This picture is also qualitatively in the spirit of phenomenological single-particle 'soft glassy rheology' trap models [38] where local strain is envisioned to induce a relative displacement of a particle from the centre of its cage formed by the surrounding particles [39]. Stress contributes a constant scalar force to the NLE of equation (1), or equivalently a linear in displacement contribution to the nonequilibrium free energy

$$F_{\rm eff}(r;\tau) = F_{\rm eff}(r;\tau=0) - fr$$
$$f = \tau\sigma^2\phi^{-2/3}, \tag{6}$$

where the microscopic force, f, is related to the macroscopic stress via the average number of particles in a unit cross-sectional area [18]. The common assumptions that the macroscopic deformation is transmitted to the particle level, and stress-induced structural and dynamical anisotropy on the local scale can be ignored, are adopted. The latter is supported by simulations of model glasses [40] and colloidal suspensions [41] which find massive shear thinning can occur with virtually no detectable anisotropy of *local* structure or dynamics, i.e. the system remains 'effectively isotropic' on the cage scale.

Within the quasi-analytic framework of the NLE theory the single-particle alpha relaxation time, τ_α, is identified with the mean first passage time over the barrier as computed from the high friction limit of Kramers' theory [16, 42]:

$$\frac{\tau_\alpha}{\tau_0} = \frac{2\pi(\zeta_{\rm s}/\zeta_0)}{\sqrt{\tilde{K}_0\tilde{K}_{\rm B}}}{\rm e}^{F_{\rm B}}, \tag{7}$$

where $\tilde{K}_0$ and $\tilde{K}_{\rm B}$ are the dimensionless (units of $k_{\rm B}T\sigma^{-2}$) absolute magnitudes of the curvature of the localization well and barrier, respectively, of $F_{\rm eff}(r)$. Applied stress distorts the effective free energy by changing the curvatures and reducing the barrier height thereby increasing the hopping rate [18]. The short time friction constant is assumed to reflect ultralocal dynamics and is taken to be independent of stress.

Equation (7) allows the alpha time as a function of stress to be computed. However, if shear rate is the control variable then a relation between stress, viscosity and shear rate (constitutive equation) is required as discussed in depth previously [18]. Since our present interest is experiments at extremely high volume fractions [26], a simple (but accurate [18]) Maxwell model for the shear viscosity is adopted

$$\eta \simeq G'(\tau)\tau_\alpha(\tau) \tag{8}$$

$$G'(\tau) = \frac{1}{60\pi^2}\int_0^\infty {\rm d}q\, q^4\left(\frac{{\rm d}\ln S(q)}{{\rm d}q}\right)^2 \times \exp[-q^2 r_{\rm L}^2(\tau)/3S(q)]. \tag{9}$$

The glassy shear modulus, G', follows from the standard Green–Kubo formula plus the MCT projection and factorization approximations [1, 36]. Stress enters solely in G' via the localization length $r_{\rm L}(\tau)$ (minimum of $F_{\rm eff}(r)$) which monotonically increases with deformation corresponding to strain softening [18]. The shear rate, $\dot\gamma$, then follows from the viscous relation $\tau = \eta(\tau)\dot\gamma$, thereby allowing the calculation of $\tau_\alpha(\dot\gamma)$.

Very recently, first of their kind measurements of the incoherent dynamic structure factor of hard sphere colloidal suspensions ($\sigma = 1.7$ μm) under high shear at the cage peak, $F_{\rm s}(q^*,t)$, have been performed at an ultrahigh volume fraction of $\phi = 0.62$ [26]. The elementary timescale is $\tau_0 \equiv \sigma^2/D_0 = 24\tau_{\rm B} = 30$ s. A wide range of shear rates were studied corresponding to dimensionless Peclet numbers in the range $Pe \equiv \dot\gamma\tau_0 = 0.005$–$1.0$. The key experimental findings relevant to our present work are the following. (1) $F_{\rm s}(q^*,t)$ decays as a simple exponential function of time. (2) As seen in many simulations [40, 41], $F_{\rm s}(q^*,t)$ and the self-diffusion constant, D, show little anisotropy (<20%) despite the observation of massive shear thinning. (3) Within experimental uncertainties the alpha time is a perfect power law of shear rate: $\tau_\alpha \propto \dot\gamma^{-0.8}$, and also $D \propto \tau_\alpha^{-1} \propto \dot\gamma^{0.8}$. (4) At the lowest $Pe = 0.005$ the alpha relaxation time is $\sim$1000 s. (5) One measurement each was performed at $\phi = 0.60$ and 0.61. Surprisingly, to within the experimental error bars these alpha times fell on top of the curve for the $\phi = 0.62$ system. (6) The experiments imply the microscopic flow curve, commonly defined as $\tau \approx \eta\dot\gamma \propto G'\tau_\alpha\dot\gamma \propto \dot\gamma^{0.2}$, is of a 'power law fluid' form with no low shear rate plateau. On the other hand, bulk rheological experiments do find a low shear rate plateau which is commonly interpreted as a dynamic yield stress [26]. Hence, the macroscopic and microscopic

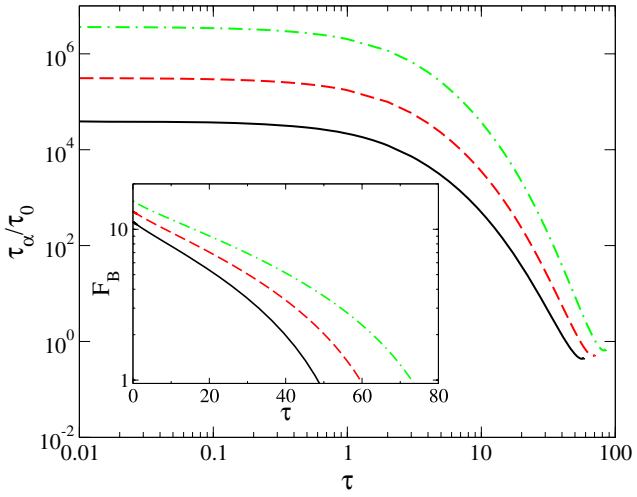

Figure 6. Dimensionless mean alpha relaxation time as a function of dimensionless stress for three volume fractions (from top) $\phi = 0.62$, 0.61, 0.60. The inset shows the corresponding entropic barrier in units of the thermal energy.

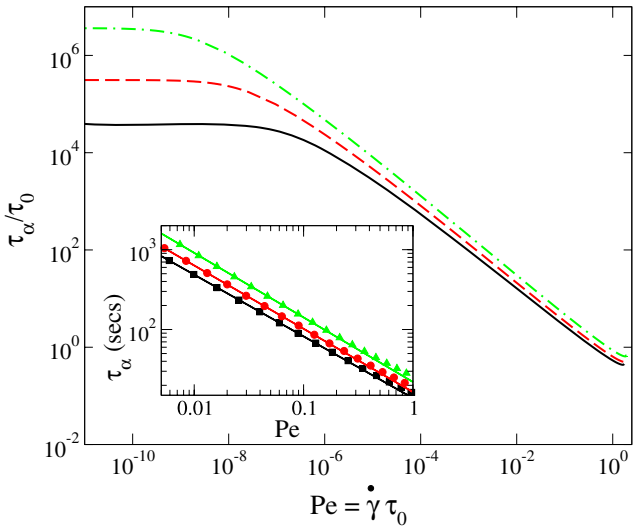

Figure 7. Log–log plot of the dimensionless mean alpha relaxation time as a function of dimensionless shear rate (Peclet number) for (from top) $\phi = 0.62$, 0.61, 0.60. Inset: expanded view of the Peclet number range relevant to recent experiments with the time axis in seconds [31]. The lines through the points are power laws $\tau_\alpha \propto \dot{\gamma}^{-x}$ where $x = 0.81$, 0.79, 0.77 for $\phi = 0.62$, 0.61, 0.60.

behaviour are not consistent, which may indicate the apparent stress plateau arises from a macroscopic rheological instability such as shear banding and localization [43, 44].

The experiment of [26] provides a unique opportunity to *directly* and *quantitatively* test the nonlinear version of the single-particle NLE theory in the *absence* of adjustable fit parameters. New calculations of the alpha time as a function of dimensionless stress (units of $k_BT\sigma^{-3}$) have been performed for $\phi = 0.60$, 0.61 and 0.62 and the results are presented in figure 6. In units of $\tau_0 \equiv \sigma^2/D_0 = 24\tau_B$, the reduced alpha time at zero stress varies by roughly two orders of magnitude from ∼20 000 to two million over this small volume fraction range. At $\phi = 0.62$ the quiescent alpha time is predicted to be astronomical, $\tau_\alpha \sim 60$ million seconds ∼ 2 years. At a dimensionless stress of order unity the relaxation time starts to decrease significantly, falling by roughly four orders of magnitude at a stress of ∼50. At high stress the differences between the alpha relaxation time for the three volume fractions becomes much smaller due to the barrier softening effect as displayed in the inset of figure 6.

Using equations (8) and (9) and $\tau = \eta(\tau)\dot{\gamma}$ the calculations in figure 6 are expressed as a function of dimensionless shear rate (Peclet number) and re-plotted in figure 7. These represent quantitative, no adjustable parameter predictions that can be directly compared with the experimental data. At $\phi = 0.62$ shear thinning begins at an exceptionally low Peclet number of $\sim 10^{-9}$. For each volume fraction, once the relaxation time has decreased by roughly an order of magnitude a power law shear thinning behaviour emerges over many decades in Peclet number. As the shear rate increases the relaxation times that were initially separated by a factor of 100 closely approach each other. If the shear rate range corresponding to $Pe = 0.0001$–1 is analysed (not plotted), then essentially perfect power law behaviour is found: $\tau_\alpha \propto \dot{\gamma}^{-x}$ with $x = 0.81$, 0.79 and 0.75 for $\phi = 0.62$, 0.61 and 0.60, respectively.

The inset of figure 7 plots our calculations over precisely the same range as experimentally studied. Essentially perfect power laws emerge with $\tau_\alpha \propto \dot{\gamma}^{-0.81}$ for $\phi = 0.62$, in accord with the experiment [26]. Over this shear rate range the apparent exponent $x = 0.79$ and 0.77 for $\phi = 0.61$ and 0.60, respectively. This remarkable agreement between theory and experiment extends to the absolute values of the mean relaxation time. Since $\tau_0 = 30$ s, the predicted alpha relaxation time at $Pe = 0.005$ is ∼800–1500 s for $\phi = 0.60$–0.62. For $\phi = 0.62$ this time is almost 5 orders of magnitude smaller than its quiescent value, and is in excellent agreement with the experimental observation of ∼1000 s at $Pe = 0.005$ [26] Finally, the theory predicts that at the Peclet numbers experimentally probed the alpha time for the three volume fractions systems are within less than a factor of two of each other. This provides an understanding of the puzzling nearly identical behaviour observed experimentally for measurements at $\phi = 0.60$, 0.61,0.62.

The level of excellent quantitative agreement between theory and experiment described above is not *a priori* expected. However, we believe it is very significant especially given there are no adjustable parameters in the comparison. In conjunction with multiple prior confrontations of the nonlinear rheological theory with experiment [18, 19], we believe there is strong support for the fundamental ideas of the NLE approach which include the relevance of entropic barriers and activated hopping [16, 27], the nonexistence of an ideal glass transition below RCP [37], and the proposed *instantaneous* Eyring-like mechanism of stress reduction of the barrier [18].

Alternative microscopic theories of the nonlinear rheology of glassy colloidal suspensions have been recently developed based on ideal MCT and the concept of shear-induced advection of density fluctuations that destroy dynamic caging constraints [45, 46]. These approaches have also had

successes. However, they are built on the nonergodic ideal glass concept (the location of which is adjusted to fit experimental data) that emerges far below RCP, and the assumed practical irrelevance of activated barrier hopping. The ideal MCT approaches predict the existence of a dynamic yield stress, in contrast to the NLE theory where ergodicity is always (in principle) restored at low enough shear rates via rare activated barrier hopping. The experiments of [26] find that the presence of a stress plateau in the bulk rheology experiment is *not* reflected in the microscopic dynamics that both MCT and the NLE theory address. Clearly more experimental work is needed to better test the various theories, and the thorny issue of macroscopic instabilities as the possible origin of yield stress plateaus must be resolved. Regardless, direct measurements of $F_s(q,t)$ or $S(q,t)$ under nonlinear flow conditions are the most definitive and appropriate tests of existing microscopic theories and hence much future experimental and simulation effort should be expended in this direction.

6. Discussion

The stochastic nonlinear Langevin equation theory of glassy single-particle dynamics of hard sphere fluids and suspensions [16, 27] has been applied to address three issues. The extent of non-Fickian (subdiffusive) behaviour at intermediate times is compared to analogous results of light scattering experiments [3, 25] with good quantitative agreement. The slow structural relaxation component of the small wavevector incoherent dynamic structure factor is calculated and overall is found to agree well with light scattering results [3, 25], although quantitative deviations do exist. The theoretical timescale for maximizing the contribution of the structural relaxation is quite similar in magnitude and volume fraction dependence to the experimental result. Various measures of non-Gaussian fluctuation effects [4, 21] have also been further analysed, including the interesting roughly power law growth, with a common exponent, of the classic and alternative non-Gaussian parameter amplitude with mean alpha relaxation time. Weak power law growth or shrinkage of several characteristic length scales are also predicted in the activated dynamics regime.

The quasi-analytic nonlinear rheology version of the theory [18] has been quantitatively applied to address recent measurements [26] of shear-induced acceleration of the single-particle relaxation time on the local cage scale. The no adjustable parameter calculations are in remarkable agreement with the experimental observations for both the absolute magnitude and power law dependence of the shear thinning phenomenon. The theory of both the linear and nonlinear bulk viscoelastic properties is based on single-particle dynamics, a simplified idea that underlies the emergent field of 'microrheology' [47]. Recent theoretical and simulation studies suggest such an approach compares remarkably well with traditional macrorheology under both quiescent and driven conditions even when the tagged particle is identical in size to the matrix particles [48]. This close correspondence between microrheology and bulk rheology provides additional support for our theoretical approach [18].

The NLE theory predicts bifurcation of the single-particle displacement distribution [21]. A full analysis of results for the van Hove function, including the exponential tail feature that is indicative of a fast hopping species, will be presented elsewhere [22]. Confrontation of the nonlinear rheology theory with experiments on dense attractive glass or gel colloidal systems is also a problem of significant interest. New experiments that measure single-particle dynamics in such gels under high stress would be exceptionally valuable to test emerging theoretical ideas.

Acknowledgments

This work was supported by the Nanoscale Science and Engineering Initiative of the National Science Foundation under NSF Award Number DMR-0642573. We thank Professor Wilson Poon and Dr Rut Besseling for helpful discussions of their experimental results in [26].

References

[1] Götze W and Sjögren L 1992 *Rep. Prog. Phys.* **55** 242
Götze W 1999 *J. Phys.: Condens. Matter* **11** A1
[2] Das S 2004 *Rev. Mod. Phys.* **76** 785
[3] van Megen W and Underwood S 1993 *Phys. Rev.* E **47** 249
van Megen W and Underwood S 1994 *Phys. Rev.* E **49** 4206
[4] Schweizer K S 2007 *Curr. Opin. Colloid Interface Sci.* **12** 297
[5] Doliwa B and Heuer A 2003 *Phys. Rev.* E **67** 030501
[6] Brumer Y and Reichman D R 2004 *Phys. Rev.* E **69** 041202
[7] Kumar S K, Szamel G and Douglas J F 2006 *J. Chem. Phys.* **124** 21450
[8] Yamamoto R and Onuki A 1998 *Phys. Rev. Lett.* **81** 4915
[9] Flenner E and Szamel G 2005 *Phys. Rev.* E **72** 031508
[10] Lowen H, Hansen J P and Roux J N 1991 *Phys. Rev.* A **44** 1169
[11] Gleim T, Kob W and Binder K 1998 *Phys. Rev. Lett.* **81** 4404
[12] Szamel G and Flenner E 2004 *Europhys. Lett.* **67** 779
[13] Berthier L and Kob W 2007 *J. Phys.: Condens. Matter* **19** 205130
[14] Reichman D R, Rabani E and Geissler P L 2005 *J. Phys. Chem.* B **109** 14654
[15] Krekelberg W K, Mittal J, Ganesan V and Truskett T M 2007 *J. Chem. Phys.* **127** 044502
[16] Schweizer K S and Saltzman E J 2003 *J. Chem. Phys.* **119** 1181
[17] Saltzman E J and Schweizer K S 2003 *J. Chem. Phys.* **119** 1197
[18] Kobelev V and Schweizer K S 2005 *Phys. Rev.* E **71** 021401
[19] Rao R, Kobelev V, Li Q, Lewis J A and Schweizer K S 2006 *Langmuir* **22** 2441
[20] Saltzman E J and Schweizer K S 2006 *J. Chem. Phys.* **125** 044509
[21] Saltzman E J and Schweizer K S 2006 *Phys. Rev.* E 061501
[22] Saltzman E J and Schweizer K S 2007 *Phys. Rev.* E in preparation
[23] Berthier L 2004 *Phys. Rev.* E **69** 020201(R)
[24] van Megen W, Mortensen T C and Williams S R 1998 *Phys. Rev.* E **58** 6073
[25] van Megen W, Mortensen T C and Bryant G 2005 *Phys. Rev.* E **72** 031402
van Megen W and Bryant G 2007 *Phys. Rev.* E **76** 021402
[26] Besseling R, Weeks E R, Schofield A B and Poon W C K 2007 *Phys. Rev. Lett.* **99** 028301
[27] Schweizer K S 2005 *J. Chem. Phys.* **123** 244501

[28] Archer A J and Rauscher M 2004 *J. Phys. A: Math. Gen.* **37** 9325
Marconi U M B and Tarazona P 1999 *J. Chem. Phys.* **110** 8032
[29] Kirkpatrick T R and Wolynes P G 1987 *Phys. Rev.* A **35** 3072
[30] Cohen E G D, Verberg R and de Schepper I M 1998 *Physica* A **251** 251
[31] Hansen J P and McDonald I R 1986 *Theory of Simple Liquids* (London: Academic)
[32] Weeks E R and Weitz D A 2002 *Phys. Rev. Lett.* **89** 095704
Weeks E R and Weitz D A 2000 *Science* **287** 627
[33] Flenner E and Szamel G 2005 *Phys. Rev.* E **72** 011205
[34] Berthier L, Biroli G, Bouchaud J-P, Kob W, Miyazaki K and Reichman D R 2007 *J. Chem. Phys.* **126** 184504
Whitelam S, Berthier L and Garrahan J P 2004 *Phys. Rev. Lett.* **92** 185705
[35] Szamel G and Flenner E 2006 *Phys. Rev.* E **73** 011504
[36] Saltzman E J and Schweizer K S 2004 *J. Phys. Chem.* B **108** 19729
[37] Schweizer K S and Yatsenko G 2007 *J. Chem. Phys.* **127** 164505
[38] Dyre J C 1987 *Phys. Rev. Lett.* **58** 792
Monthus C and Bouchaud J P 1996 *J. Phys. A: Math. Gen.* **29** 3847
[39] Evans R M L, Cates M E and Sollich P 1999 *Eur. Phys. J.* B **10** 705
Sollich P 1998 *Phys. Rev.* E **58** 738
[40] Yamamoto R and Onuki A 1998 *Phys. Rev.* E **58** 3515
Miyazaki K, Yamamoto R and Reichman D R 2004 *Phys. Rev.* E **70** 011501
[41] Foss D R and Brady J F 1999 *J. Fluid Mech.* **401** 243
[42] Kramers H A 1940 *Physica* **7** 284
[43] Varnik F, Bocquet L and Barrat J-L 2003 *Phys. Rev. Lett.* **90** 095702
[44] Coussot P, Raynaud J S, Bertrand F, Moucheront P, Guilbaud J P, Huynh H T, Jarny S and Lesueur D 2002 *Phys. Rev. Lett.* **88** 218301
[45] Miyazaki K and Reichman D R 2002 *Phys. Rev.* E **66** 050501
[46] Fuchs M and Cates M E 2002 *Phys. Rev. Lett.* **89** 248304
Fuchs M and Cates M E 2003 *Faraday Discuss* **123** 267
Brader J M, Voightmann T, Cates M E and Fuchs M 2007 *Phys. Rev. Lett.* **98** 058301
[47] MacKintosh F C and Schmidt C F 1999 *Curr. Opin. Colloid Interface Sci.* **4** 300
[48] Carpen I C and Brady J F 2005 *J. Rheol.* **49** 1483
Khair A S and Brady J F 2006 *J. Fluid Mech.* **557** 73